

THE COMPASS SPECTROMETER: STATUS AND PERFORMANCE

S. Dalla Torre

INFN, Sezione di Trieste, Italy

Abstract

The status and performances of the COMPASS spectrometer at the end of the first year of data taking, namely September 2002, is reviewed in detail. Particular attention is paid to the innovative aspects of the apparatus, which are essential to fulfil the whole COMPASS physics programme in the COMPASS critical environment (high beam fluxes, high trigger rates and quite crowded events); these aspects have also the merit of opening the way to future experimental studies in similar extreme conditions.

1. INTRODUCTION

The COMPASS Collaboration, consisting of more than 200 physicists from 26 Institutions from all over Europe, Russia, Japan, Israel and India is performing the experiment NA58, an experiment devoted to hadron physics at the CERN SPS [1]; this scientific goal is pursued with a rich, twofold research programme (as already indicated in the Collaboration acronym: Common Muon and Proton Apparatus for Structure and Spectroscopy):

- Nucleon spin structure, with particular emphasis on:
 - Gluon polarization $\Delta G(x)/G(x)$
 - Flavour-separated polarized distribution functions $\Delta q(x)$
 - Transverse-spin distribution functions $\Delta_T q(x)$
 - Spin-dependent fragmentation ΔD_q^Λ
- Spectroscopy items, and more precisely:
 - Primakoff reactions
 - Polarizability of π and K
 - Glueballs and hybrids
 - Semileptonic decays of charmed mesons and baryons
 - Double-charmed baryons.

Nucleon spin structure measurements are performed using the SPS polarized muon beam scattered off polarized nucleon targets; the spectroscopy programme foresees the use of secondary hadron beams and a variety of targets, including some cryogenic ones. While beam and targets are different for the various measurements, the large majority of the spectrometer detectors are common to both physics programmes. The present status of the experimental apparatus and its actual performances are discussed in the following sections. Up to now, the experiment has collected data with muon beam for polarized deep-inelastic scattering (DIS) measurements: in discussing the status, some reference to items specific to this part of the research programme (like the polarized target) and to performances with muon beam are given.

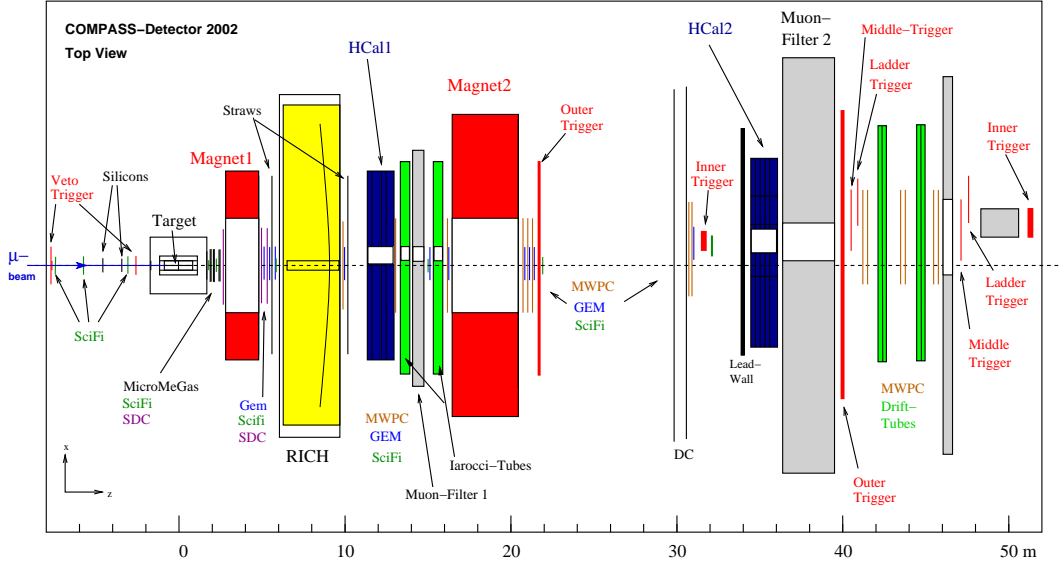


Fig. 1: The COMPASS spectrometer, top view.

2. THE SPECTROMETER LAY-OUT

The COMPASS experimental apparatus (Fig. 1) is a two-stage spectrometer, namely a Large Angle Spectrometer (LAS), placed immediately downstream of the target to allow for wide angular acceptance (± 180 mrad) and the Small Angle Spectrometer (SAS), downstream of the first one. In the original design, both spectrometers were equipped with analysing magnets (SM1, bending power: 1 Tm; SM2, bending power: 4 Tm), trackers telescopes, electromagnetic and hadronic calorimeters, muon filters and a RICH for hadron identification. Presently, for the first phase of the experiment, the spectrometer on floor includes most of this set-up, while part of the large-area trackers of the second spectrometer, the read-out electronics of the electromagnetic calorimeters and RICH-2, foreseen for hadron PID in SAS, are missing. The COMPASS Collaboration is now considering the completion of the spectrometer.

The spectrometer extends over a total length of ~ 60 m and several detectors have quite considerable transversal dimensions. These dimensions have imposed the construction of several relevant mechanical structures, as, for instance, the ones shown in Figs. 2, 3 and 4.

3. THE POLARIZED TARGET

The COMPASS polarized target [2] is formed of two cells, each 60 cm long, housing the target material, with opposite polarization. The heart of the system is formed by the ^3He - ^4He dilution refrigerator that allows the target material to be kept at a temperature well below 1 K (typically: 50 mK) and the superconducting solenoid, designed to provide 2.5 T field with homogeneity at 10^{-4} level. The COMPASS solenoid, a new superconducting magnet with wide aperture to ensure ± 180 mrad acceptance for the first spectrometer is not yet available: its construction by industry has, so far, not been successful; present perspectives for the successful construction of the COMPASS solenoid are quite favourable. Presently, the COMPASS polarized target makes use of the excellent solenoid built for the polarized target (Fig. 5) of the SMC experiment, with field homogeneity within 2×10^{-5} : the acceptance is reduced to ± 70 mrad. Both the SMC magnet and the future COMPASS one can also provide a transverse magnetic field (up to 0.5 T) to make possible target transverse polarization, for key measurements included in the COMPASS physics programme.

The target material used so far is irradiated ^6LiD , a material characterised by an extremely favourable dilution factor ($\sim 50\%$) and which allows for very high values of nucleon polarization. The COM-

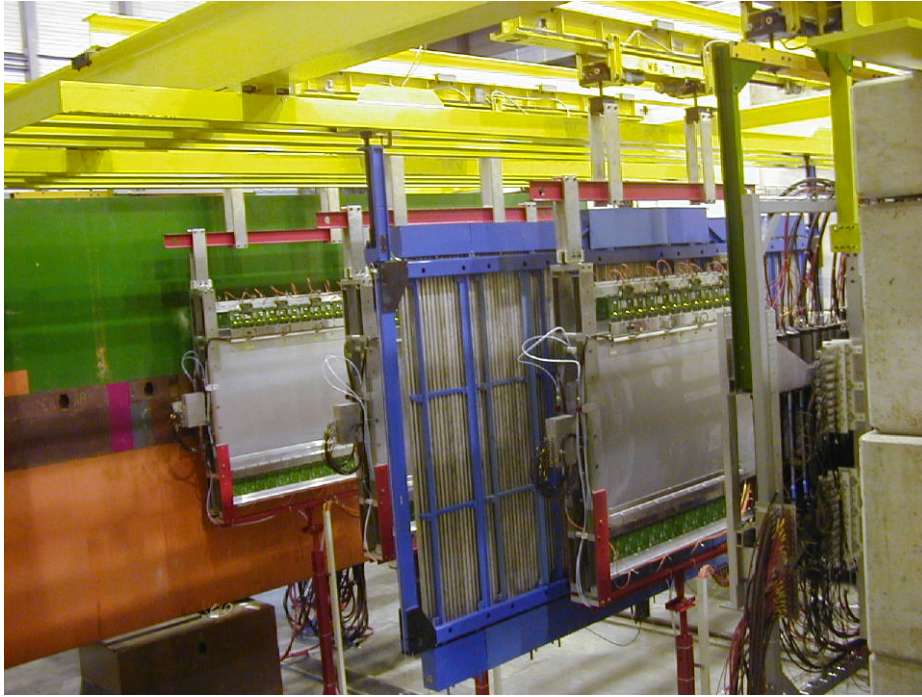


Fig. 2: The support of some tracking detectors in the region of Muon Wall 2; two stations of MWPCs and one of steel drift tubes are visible.



Fig. 3: The large frame of the electromagnetic calorimeter ECAL1.

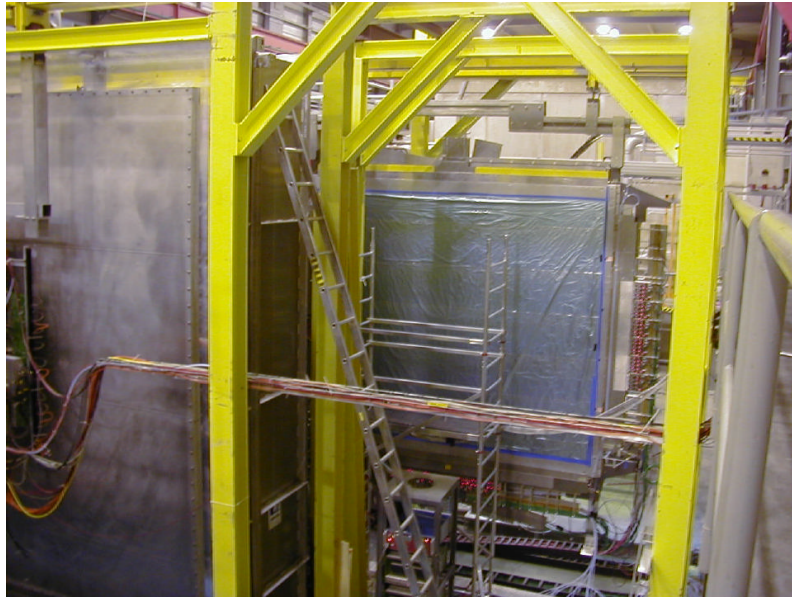


Fig. 4: The support structure of the large area trackers in the RICH-1 region allowing trackers to be rolled in the on-beam position and out for maintenance interventions; the RICH vessel is also partially visible.

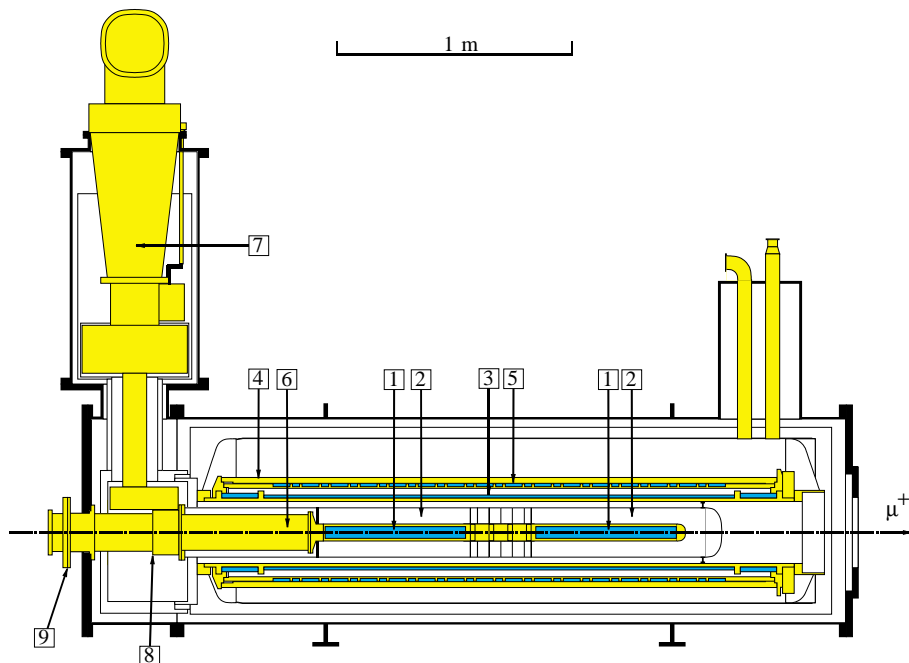


Fig. 5: The SMC target cryostat with the target holder as used in 1993 (from Ref. [3]). (1) target cells, (2) microwave cavity, (3) solenoid coil, (4) dipole coil, (5) correction coils, (6) dilution refrigerators, (7) precooler of ^3He , (8) indium seal, and (9) external seal.

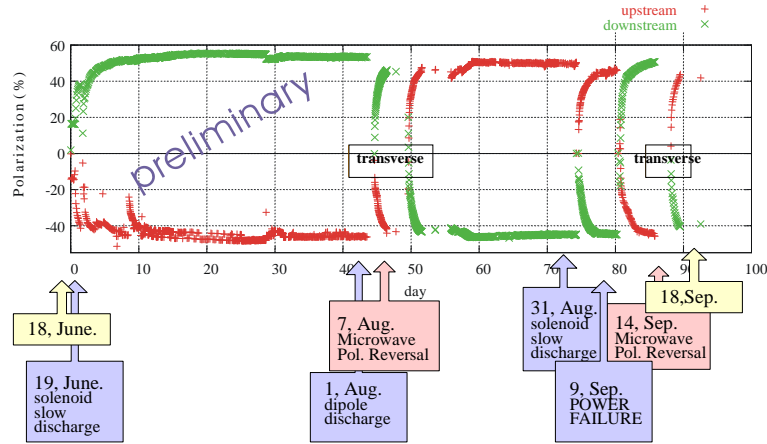


Fig. 6: The measured polarization (preliminary) in the upstream (+) and downstream (x) target cell respectively during the 2002 run; the polarization cannot be measured during transverse spin orientation.

PASS polarized target is the first large-scale one in which this material is used. A world polarization record at 2.5 T was obtained in 2001: -47% in one cell and $+54\%$ in the other one. In 2002, the quite satisfactory performance of the polarized target during the whole run (Fig. 6) confirms that the instrument is not only adequate for making records, but it is a reliable tool for good physics measurements.

The spin relaxation time in longitudinal mode (2.5 T) is too long to be measured, in transverse spin mode (0.4 T), it is longer than 1000 h. When target polarization is transversally aligned, the frozen spin mode is the only possible operational mode, a mode in which the target polarization cannot be monitored continuously: this long relaxation time is a prerequisite for the data taking with transverse target polarization. About 24% of the 2002 data-taking period was dedicated to collecting data with transverse orientation of the target polarization.

4. THE TRACKERS OF THE COMPASS SPECTROMETER

The requirements for the performance of the trackers are quite different at different distances from the beam axis: three families of trackers are present in the spectrometer: the Very Small Area Trackers (VSAT), the Small Area Trackers (SAT) and the Large Area Trackers (LAT), illustrated in the following sections.

4.1 The very small area trackers

In the very central region, only technologies capable of standing extremely intense beams can be employed; moreover good time-resolution capabilities are needed to disentangle the information from the event of interest from that of the preceding and following ones.

The **Beam Momentum Station (BMS)** makes possible the measurement of the incoming particle momentum on an event-by-event base. It consists of an analysing magnet which separates the particles, according to their momenta, in the vertical plane, and four hodoscopes of scintillator counters, with horizontal elements and granularity of 5 mm. The hodoscopes are from previous experiments at the SPS muon beam line, will the high-voltage power supply and the TDC read-out is a new COMPASS installation. The achieved time resolution is ~ 300 ps, the BMS overall efficiency is $\sim 90\%$ and the momentum resolution is better than 0.7% at 160 GeV/c.

A system of 9 stations of **scintillating fibre hodoscopes** [4] (Figs. 7 and 8) allows the measurement of 21 coordinates along the beam line, upstream and downstream of the target. These detectors have an enormous rate capability: up to 5 MHz per fibre. The total system includes 2668 fibre channels and

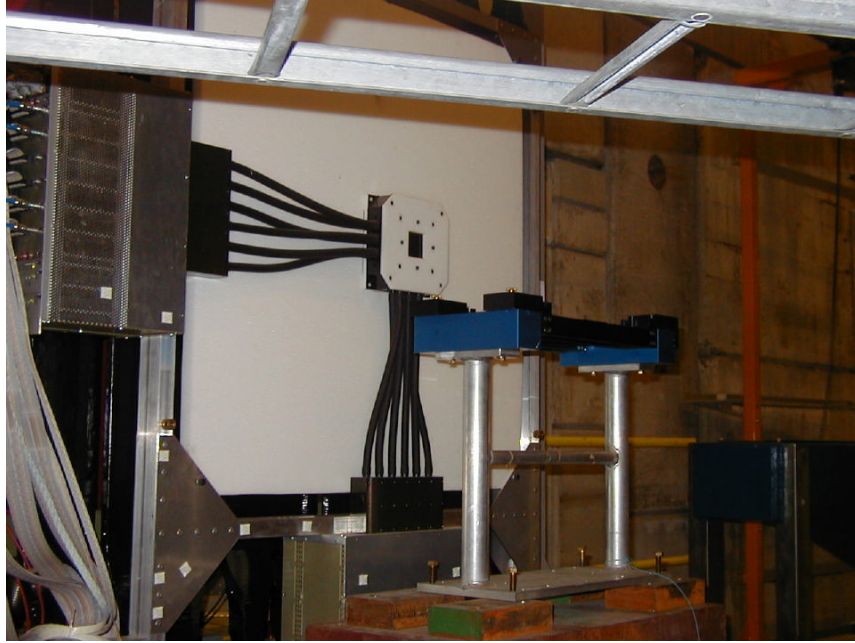


Fig. 7: One of the scintillating fibre stations installed in the COMPASS spectrometer; clear fibres connect the active region and the multianode PMTs, located far from the beam line.

4008 discriminator channels. Fibre diameters range from 0.5 to 1 mm. Fibre material is SCSF-78MJ by Kuraray Corporation. Fibres are read by multianode photomultiplier tubes H6568 from Hamamatsu. Particles to be detected cross typically 3–3.5 mm of scintillating material, thanks to the multiple layer arrangement of the fibres. The typical efficiency is $\sim 99\%$, while time resolution ranges between 350 and 550 ps (Fig. 9). Space resolution is also quite good: 130 μm or 250 μm , according to the different fibre diameters.

Two stations of **silicon strip detectors** (Figs. 10 and 11), four views each, having $50 \times 70 \text{ mm}^2$ surface, with 50 μm pitch, complement the tracking of the incoming beam trajectories. They exhibit high efficiency ($\sim 99\%$) and 3 ns time resolution (Fig. 12) (see Ref. [5] for more details).

4.2 The small area trackers

These tracking detectors cover a region of $\sim 20 \text{ cm}$ from the beam axis, with the exclusion of the central region, where the particle rate is very high ($\sim 3 \text{ cm}$ with respect to the beam axis). Two different types of novel gaseous detectors are used in COMPASS for the small area tracker set-up: they are micromegas [6] (micromesh gaseous detectors) and GEM detectors [7] (see Fig. 13 for a schematic description of the basic detector principle and Fig. 14 for a picture of a typical GEM foil). For both types, we have, in the COMPASS spectrometer, the first installation of large surface units.

Micromegas detectors form, in the COMPASS spectrometer, a telescope of 3 stations (Figs. 15 and 16), for a total number of 12 measured coordinates; the active surface is $40 \times 40 \text{ cm}^2$ with a central dead zone of 5 cm in diameter. They form a telescope placed between the target and the first analysing magnet SM1. They have a typical space resolution of 70 μm , time resolution better than 10 ns and efficiencies larger than 97%.

The **GEM** system consists of 10 stations, each equipped with two detectors for the measurement of 4 coordinates (each detector has two-dimensional read-out elements); the detector surface is $30 \times 30 \text{ cm}^2$, with a central circular dead zone with 4 cm diameter. Space resolution is $\sim 50 \mu\text{m}$, time resolution $\sim 12 \text{ ns}$ and typical efficiency in the range 96–97% [8].

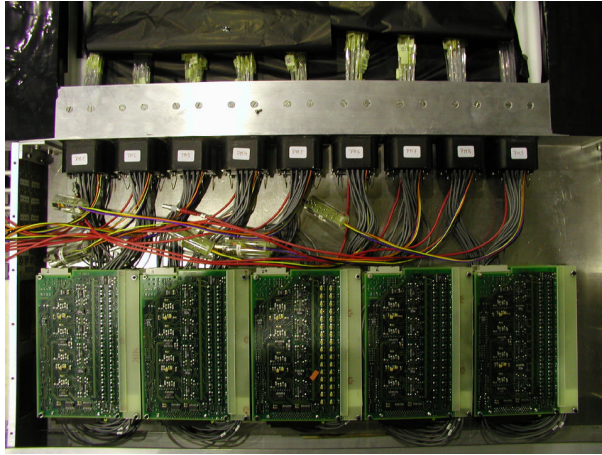


Fig. 8: Terminal edge of the clear fibres, multianode PMTs and the front-end electronics of one of the scintillating fibre stations installed in the COMPASS spectrometer.

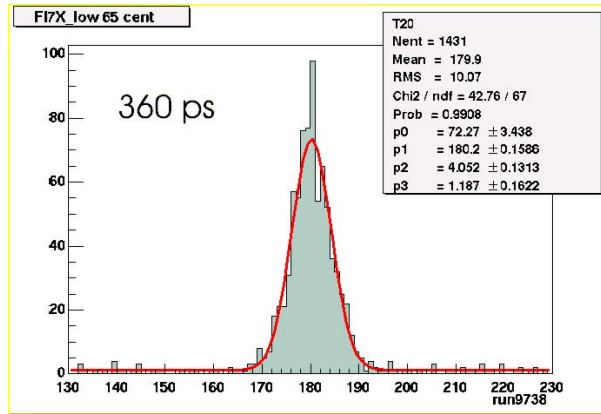


Fig. 9: Time resolution of one of the COMPASS scintillating fibre hodoscopes: 360 ps has been obtained for this unit.

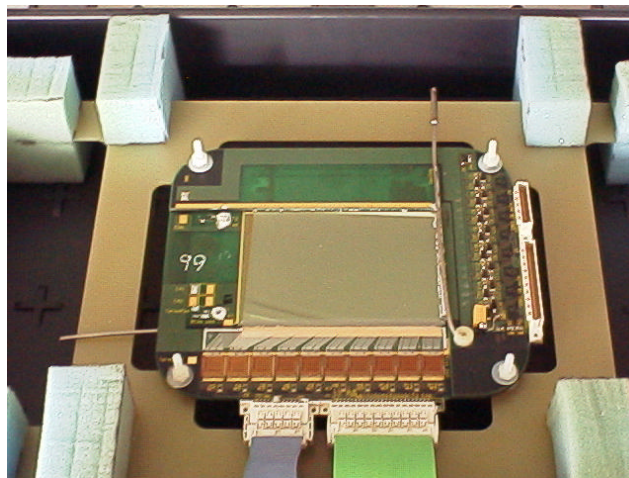


Fig. 10: One of the silicon strip detectors used for beam particle tracking in the COMPASS spectrometer.

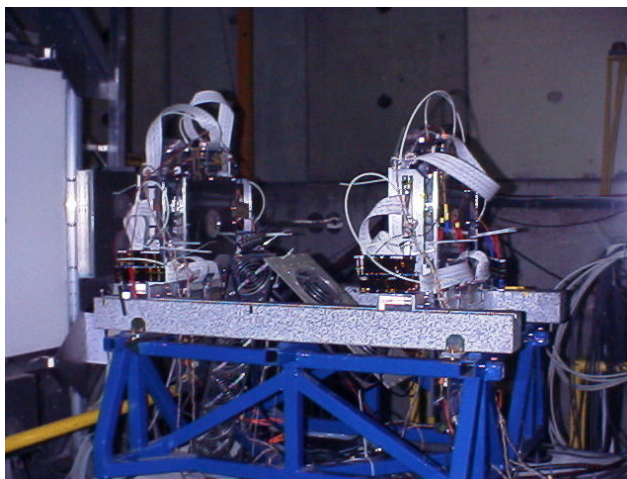


Fig. 11: The two stations of silicon strip detectors measuring incoming beam trajectories in the COMPASS spectrometer.

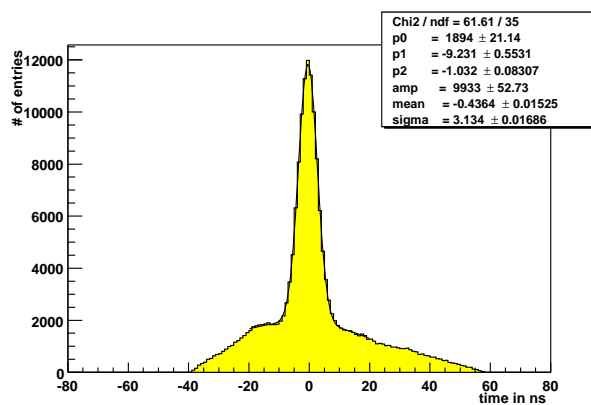


Fig. 12: Time resolution of the COMPASS silicon strip detectors.

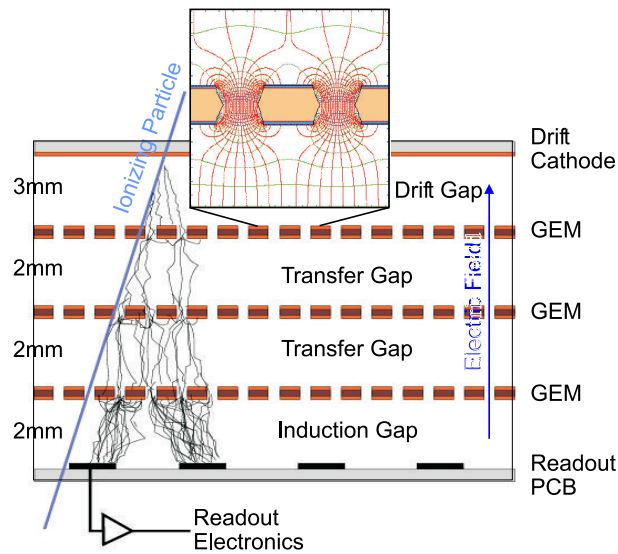


Fig. 13: Working principle of GEM detectors. At each GEM foil, charge multiplication is obtained applying a potential difference between the two faces of the foil itself (see the frame showing a zoom of the GEM foil); the total detector gain is obtained with a set of three foils.

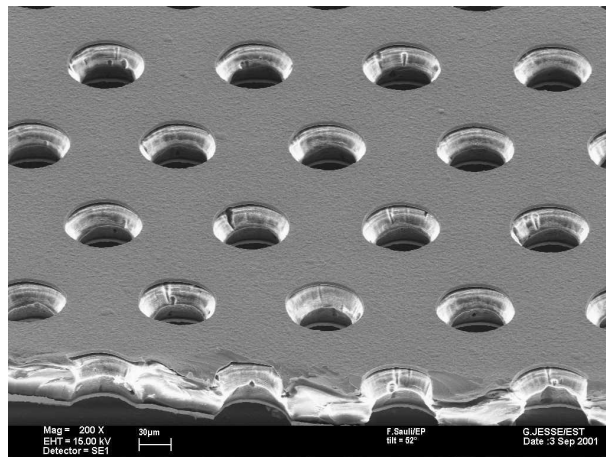


Fig. 14: Picture of a GEM foil.

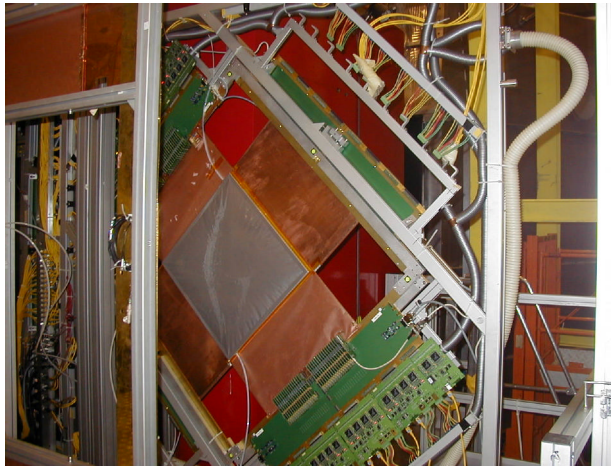


Fig. 15: One of $40 \times 40 \text{ cm}^2$ micromegas built for the COMPASS spectrometer.



Fig. 16: The micromegas telescope installed in the COMPASS spectrometer.

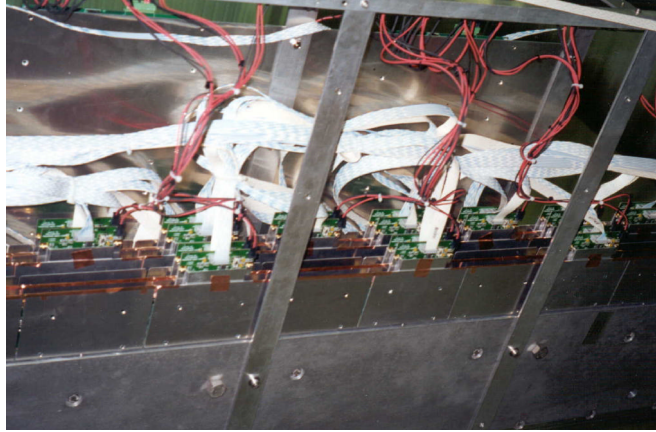


Fig. 17: The front-end cards of the drift chambers W4-5.

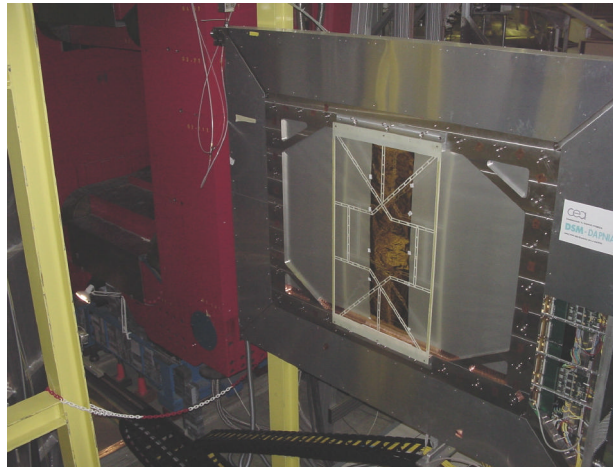


Fig. 18: One of the three SDC drift chamber detectors installed in the COMPASS spectrometer; the support of one of the GEM stations is also visible.

4.3 The large-area trackers

Telescopes of large-area trackers (all with surfaces of several m^2) are formed by detectors with four different designs, some of them are new detectors, namely drift chambers SDC and straw tube planes, others come from previous experiments and have been refurbished: MWPCs from the OMEGA spectrometer and the large drift chambers W4-5, from the SMC experiment. The read-out systems of the refurbished detectors are completely new, designed to match the basic requirements of the COMPASS data acquisition system (see Fig. 17 and Section 8).

The **SDC system** includes three drift chamber stations (Fig. 18), each measuring 8 coordinates with 7 mm drift cells; the space resolution is $\sim 170 \mu\text{m}$ (Fig. 19) and the efficiency ranges between 95% and 99.8%.

The **COMPASS straw tube** telescope includes 15 Double Layer (DL) planes ($2.3 \times 1.6 \text{ m}^2$) of tubes, 6 mm diameter and 10 mm diameter at the plane external edges [9] (Fig. 20). Nine DL planes were operational in 2002, while now all 15 DL are installed in the spectrometer. The straw tube planes have a space resolution $\sim 270 \mu\text{m}$ and efficiencies ranging between 85% and 98%.

The largest tracking set in SAS is formed by 11 **MWPC stations**, for a total amount of 34 planes

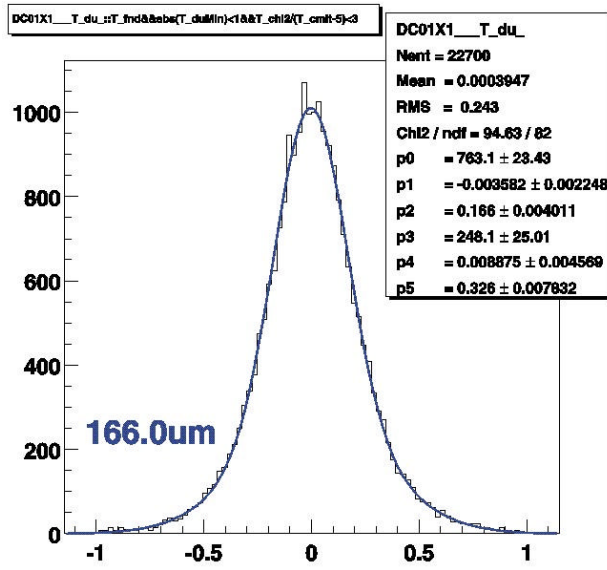


Fig. 19: Typical space resolution ($166 \mu\text{m}$ in this example) of the SDC planes.



Fig. 20: A straw detector double layer mounted in the COMPASS set-up; the aluminium-coated Mylar protective foil, which separates the dry atmosphere surrounding the tube and the external atmosphere, and the front-end read-out electronics are visible.

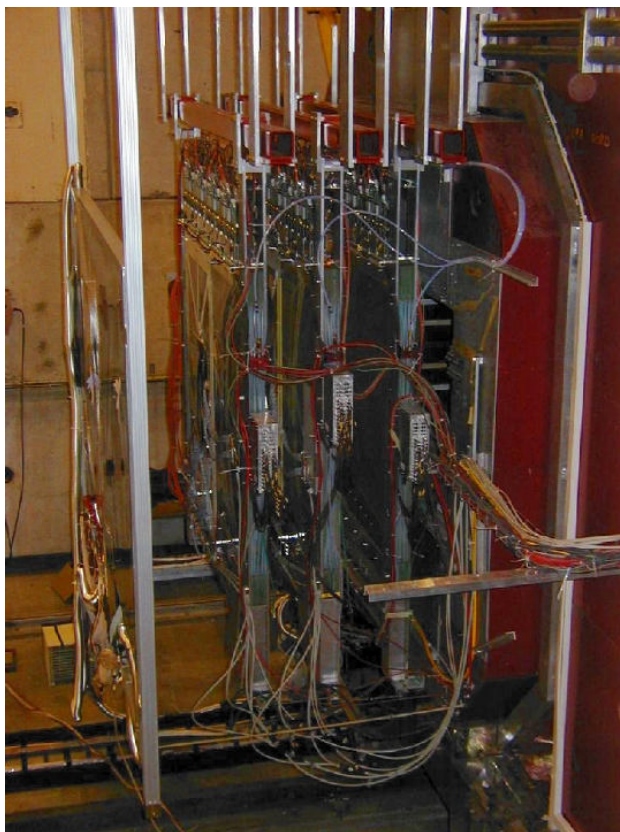


Fig. 21: Three of the 11 MWPC stations included in the COMPASS spectrometer.

of 2 mm pitch anode wires. These detectors, fully operational in 2001, exhibit a mean efficiency of 99.3%. MWPC trackers, previously used in the OMEGA spectrometer at CERN SPS, have been fully refurbished introducing a central dead zone to make them compatible with COMPASS high beam rates. Three stations are visible in Fig. 21.

Two large size drift chambers, named **W4-5**, were added to the COMPASS set-up in 2002 (Fig. 22). These detectors open the possibility of measurements at large Q^2 and made possible the first data taking with a transversely polarized target during the 2002 run. More W4-5 stations will be available for the 2003 run and the access to the large Q^2 domain will be completed by other large-area trackers under discussion in the context of the completion of the COMPASS spectrometer.

5. COMPASS CALORIMETRY

Both COMPASS spectrometers are equipped with electromagnetic and hadron calorimeters: ECAL1 and HCAL1 in the LAS, ECAL2 and HCAL2 in the SAS.

Both, HCAL1 and HCAL2, are sandwich type calorimeters made up of iron converters and scintillator plates. The light collection is performed with wave-length-shifting fibres. These two calorimeters are fully mounted and instrumented. Their measured resolution is

- HCAL1 (Fig. 23)

$\sigma/E = 59.4\%/\sqrt{E} \oplus 7.6\%$	for π
$\sigma/E = 24.3\%/\sqrt{E} \oplus 0.6\%$	for e^-
- HCAL2:

$\sigma/E = 65\%/\sqrt{E} \oplus 4\%$	for π .
---------------------------------------	-------------

The electromagnetic calorimeters are not yet operative. ECAL1 is made up of lead glass blocks from previous GAMS and OLGA calorimeters; all blocks are available, the calorimeter support is in

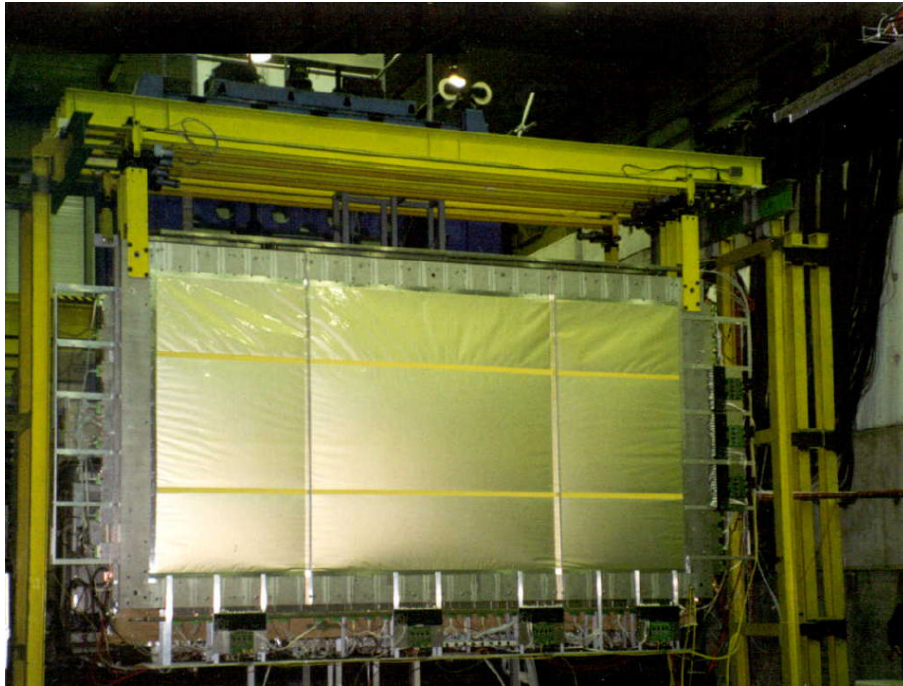


Fig. 22: Front of one of the drift chambers W4-5.

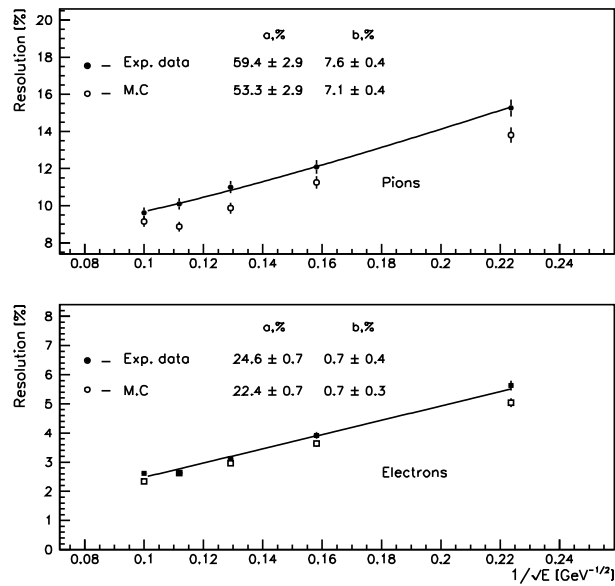


Fig. 23: The measured HCAL1 resolution for pions (upper plot) and for electrons (lower plot).

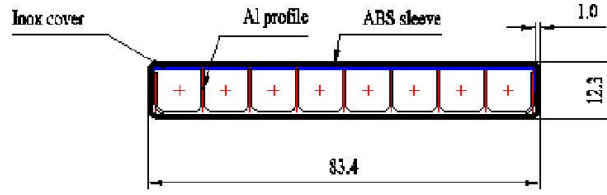


Fig. 24: The basic geometry of the Muon Wall 1 trackers: they are aluminium ‘Iarocchi tube’ detectors.

production. The known resolution of the OLGA calorimeter is $\sigma/E = 5.8\%/\sqrt{E} \oplus 2.3\%$. ECAL2 is made up of blocks from GAMS to be complemented by sandwich type elements (of either the pappardelle or Shashlik type); the LG blocks are presently mounted and partially instrumented.

6. PARTICLE IDENTIFICATION IN COMPASS

Muon identification is performed with muon filters, while hadron identification is pursued with RICH detectors. RICH-1, equipping LAS, is already operative while RICH-2, the high momentum partner, which will complete SAS, is one of the major projects foreseen for the completion of the spectrometer.

6.1 The muon walls

Muon filters are implemented in both spectrometers: Muon Wall 1 (LAS) and Muon Wall 2 (SAS). The detectors of Muon Wall 1 are planes ($4 \times 2 \text{ m}^2$) of aluminium ‘Iarocchi tubes’ (the basic geometry is presented in Fig. 24, while a picture of the detectors is given in Fig. 25). They sandwich a 60 cm thick iron absorber. The detectors employed in Muon Wall 2 are planes of 3 cm diameter steel drift tubes; the absorber, 2.4 m thick, is formed of concrete blocks.

6.2 COMPASS RICH-1

RICH-1 [10] has been designed to separate π 's and K's with momenta up to $\sim 60 \text{ GeV}/c$ in a high-intensity environment and to cover the full acceptance of the large-angle spectrometer. The material has been minimised to preserve the tracking resolution of the small-angle spectrometer and the energy resolution of the downstream electromagnetic and hadronic calorimeters. The main parameters achieved are:

- **RADIATOR**: A 3 m long C_4F_{10} radiator at atmospheric pressure, with a contamination of oxygen and moisture kept below 5 ppm, to have a transmittance higher than 80% for 165 nm photons, for a typical path length of 4.5 m.
- **VESSEL**: For the vessel ($\sim 80 \text{ m}^3$) non polluting materials were used, mainly aluminium. The incoming leakage rate is $\sim 3 \text{ Pa} \times \text{l/s}$.
- **MIRRORS**: The mirror system consists of spherical mirrors, radius of curvature 6.6 m, segmented in 116 hexagonal and pentagonal pieces covering a total area $> 20 \text{ m}^2$ (Fig. 26). Two spherical surfaces focus the Cherenkov photons onto two sets of photon detectors placed above and below the acceptance region. These mirrors have a local deviation of the shape from the spherical $\sigma_\theta < 0.2 \text{ mrad}$, a maximum deviation from the nominal radius of curvature $\delta_R/R = 0.5\%$ and a reflectance $> 80\%$ down to 165 nm.
- **PHOTON DETECTOR**: Taking into account the large area to be instrumented (5.3 m^2) and the need for a pixel size of $\sim 1 \text{ cm}$, MWPCs with segmented CsI photo-cathodes were chosen. These UV photon detectors were developed in the context of RD26 [11] and, later, for the ALICE HMPID project [12], and adopted for several other projects [13]. RICH-1 is equipped with 8 identical

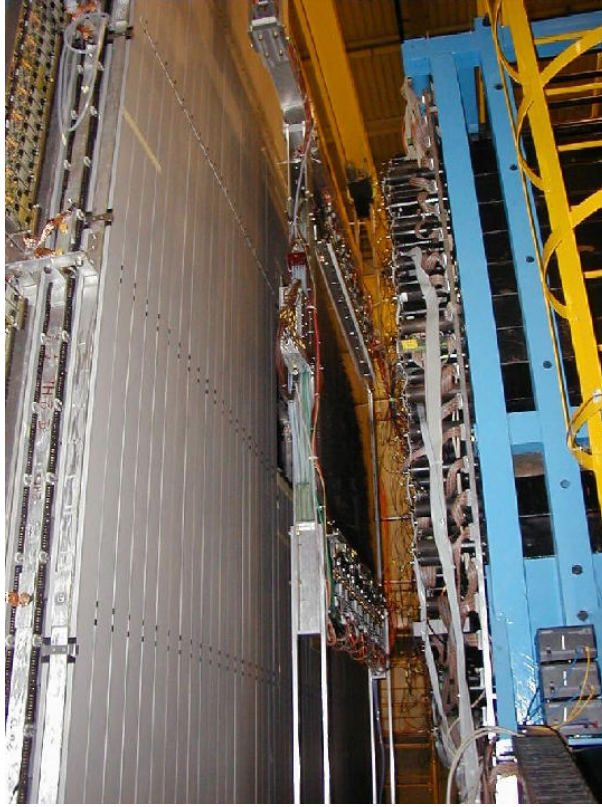


Fig. 25: Muon Wall 1: the muon filter of the Large Angle Spectrometer.

chambers, each one having an active surface of $576 \times 1152 \text{ mm}^2$ (Fig. 27). Two $576 \times 576 \text{ mm}^2$ double-layer PCBs, each segmented in 5184 $8 \times 8 \text{ mm}^2$ pads, coated with CsI form the photocathode planes (for more details about the coating technique see Ref. [14]). Silica quartz windows ($600 \times 600 \times 5 \text{ mm}^3$) separate the radiator from the photon detectors.

- **FRONT END ELECTRONICS** The 82 944 channels, equipped with analog readout electronics, correspond to $\sim 40\%$ of the total number of channels of the experiment.
- **MATERIAL BUDGET:** The total radiation length is 22.5% of X_0 . The major contributions to the material budget in the acceptance is given by the radiator (10.5% of X_0); the other contributions are quite reduced: the mirror substrates (5.5% of X_0), the mirror mechanical supports (2.5% of X_0) and the front and rear vessel windows (2% of X_0 each). In the beam region, where a He-filled pipe is used, particles have to cross only 1.6% of X_0 .

Figure 28 shows an event from the RICH on-line event display. The preliminary resolution of the measured Cherenkov angle resolution for ultrarelativistic particles is 0.4 mrad (Fig. 29); a flavour of the RICH performances is presented in Fig. 30.

7. THE COMPASS TRIGGER FOR THE DEEP INELASTIC SCATTERING PROGRAMME

The set-up forming the COMPASS trigger for the DIS programme (Fig. 31) consists of almost 500 dedicated scintillator counter channels, viewed by PMs, read via dedicated, custom discriminator boards. Mean-timer circuits are used for those scintillator strips, which, because of their length, are equipped with PMs at both ends. Custom mean-timer boards allow to form correlations between different hodoscopes in an extremely short time. The COMPASS trigger for the DIS programme is based on the correlation of the information from different hodoscopes in order to select scattered-particle trajectories originating from the target. To increase the trigger purity, in particular in the small Q^2 domain, the information from

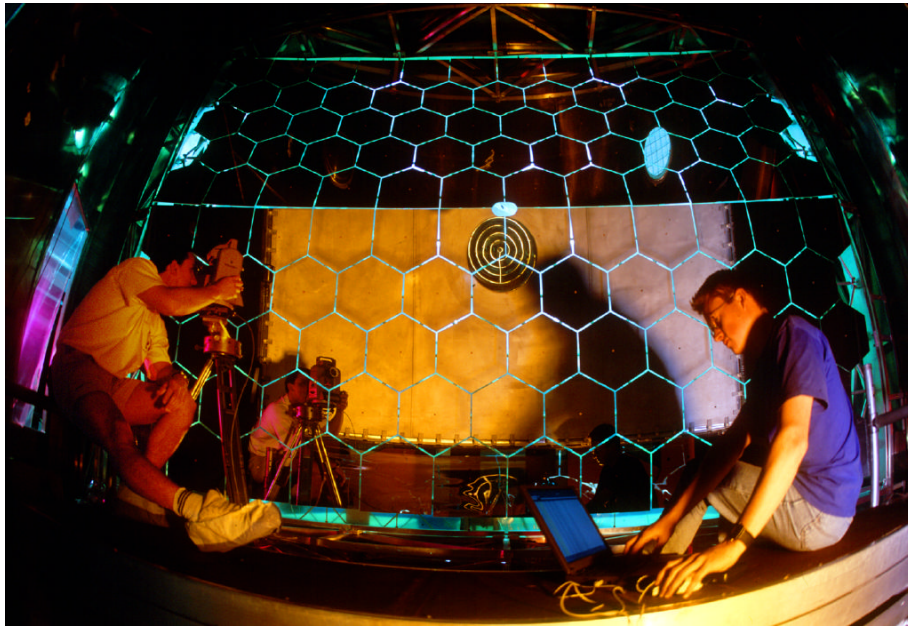


Fig. 26: The mirror wall during the alignment of the mirrors.

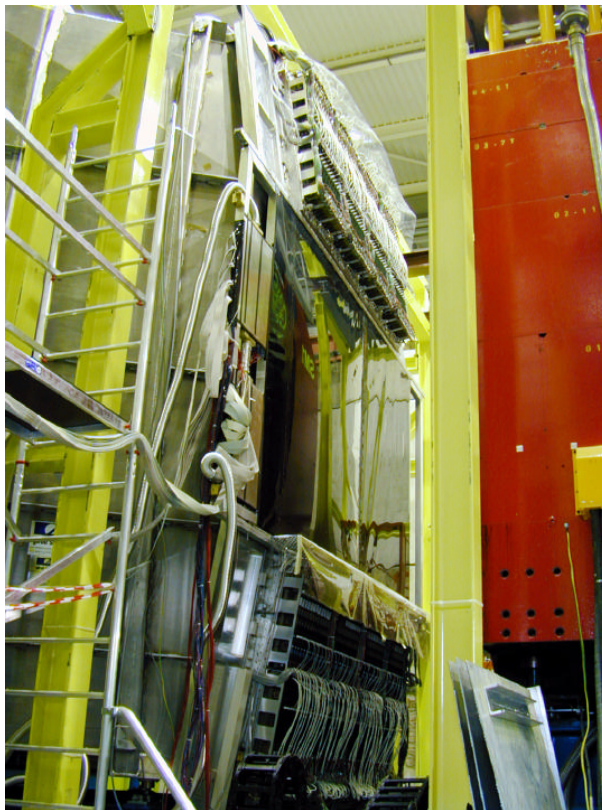


Fig. 27: RICH-1 upstream side: the photon detectors, top and bottom sets, fully equipped with read-out electronics are visible.

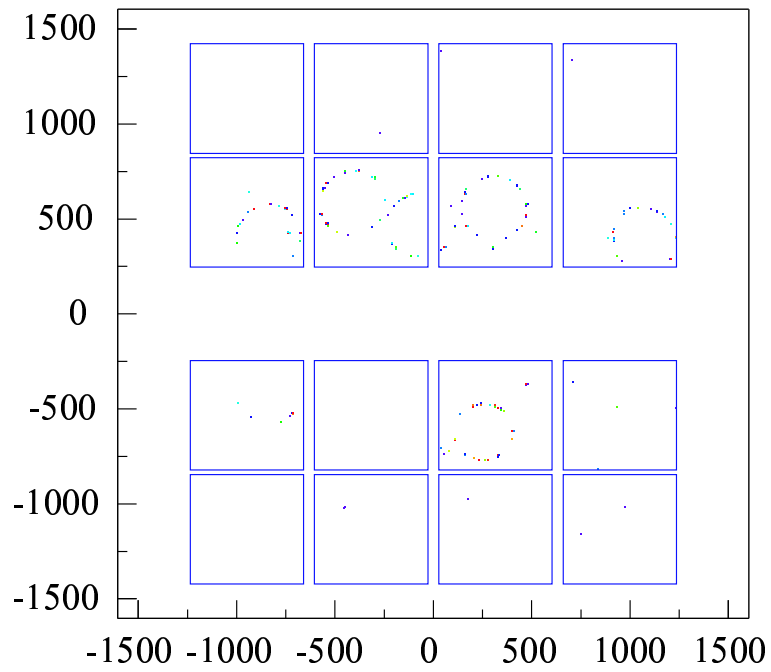


Fig. 28: An event from the RICH on-line event display.

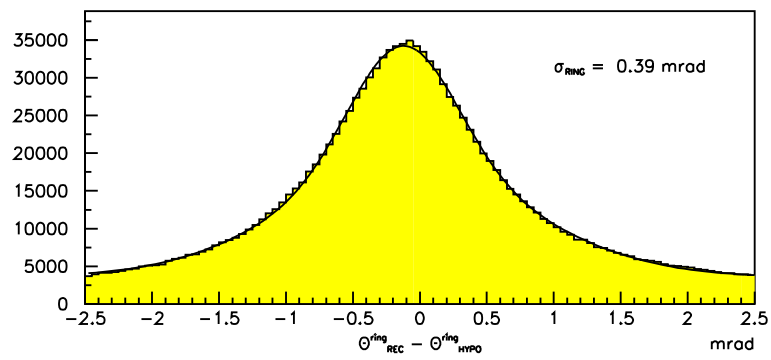


Fig. 29: Preliminary resolution of the measured Cherenkov angle for ultrarelativistic particles.

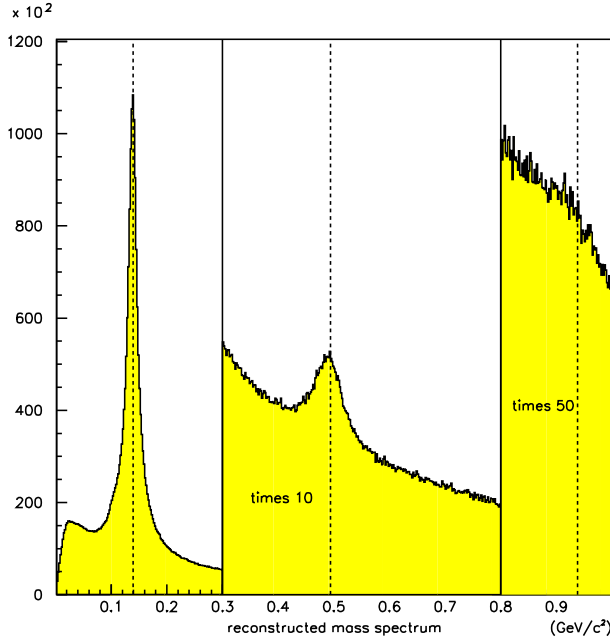


Fig. 30: Preliminary mass spectrum obtained with COMPASS RICH-1; π and K peaks are clearly visible; there is also an indication of a proton signal.

the hodoscopes is complemented with that of the hadron calorimeters (Fig. 32). Different combinations of hodoscope information allow the various kinematical regions to be spanned (Fig. 33).

8. FRONT-END ELECTRONICS AND DATA ACQUISITION

The 191 000 electronic channels of the COMPASS spectrometer are read by a read-out system characterised by its pipelined architecture and by a design which makes it fully extendible [15]. An overall scheme of the COMPASS read-out and data acquisition system is presented in Fig. 34.

Different front-end chips are used (such as a SFE16 preamplifier-discriminator for the micromegas, APV25 for GEMs and silicon detectors, MAD4 and ADS8 for large area trackers, COMPASS-GASSI-PLEX for RICH-1 read-out). The front-end and digitising boards (based, for the conversion to digital information, on chips like F1-TDC [16] for several trackers, FIADC for calorimetry and AD 9201ARS for RICH-1) transfer the information to custom VME boards (CATCHes [16] for most of the detectors, GeSiCA for GEMs and silicon trackers). In particular, RICH front-end BORA boards [17] perform a first sparsification and data reduction stage thanks to the use of distributed intelligence: each front-end board is equipped with a powerful DSP and an FPGA. From VME boards, data are transferred via optical S-links to large memory buffers, spill buffers, hosted in PCs, where the data of a whole burst are stored. The SPS duty cycle is $\sim 25\%$: the use of large-memory spill buffers allows the whole SPS cycle to be used to increase the effective bandwidth downstream of the buffers themselves. All the electronics read-out components from front-end to spill buffers are custom designed.

The Data Acquisition System (DAQ) (Fig. 35), downstream of the large memory buffer, is based on commercial devices: its heart is the Gigabit Ethernet Switch, which allows the information to be distributed from the spill buffers to a net of 12 event-builder PCs. The DAQ software is based on ALICE DATE.

The present performances of the overall read-out and DAQ system can be summarised by the following figures: at ~ 5 kHz trigger rate over the spill duration (~ 5 s), the read-out and DAQ dead time is 7%, while the typical event size is ~ 40 kB, corresponding to data rates of 220 MB/s during spill,

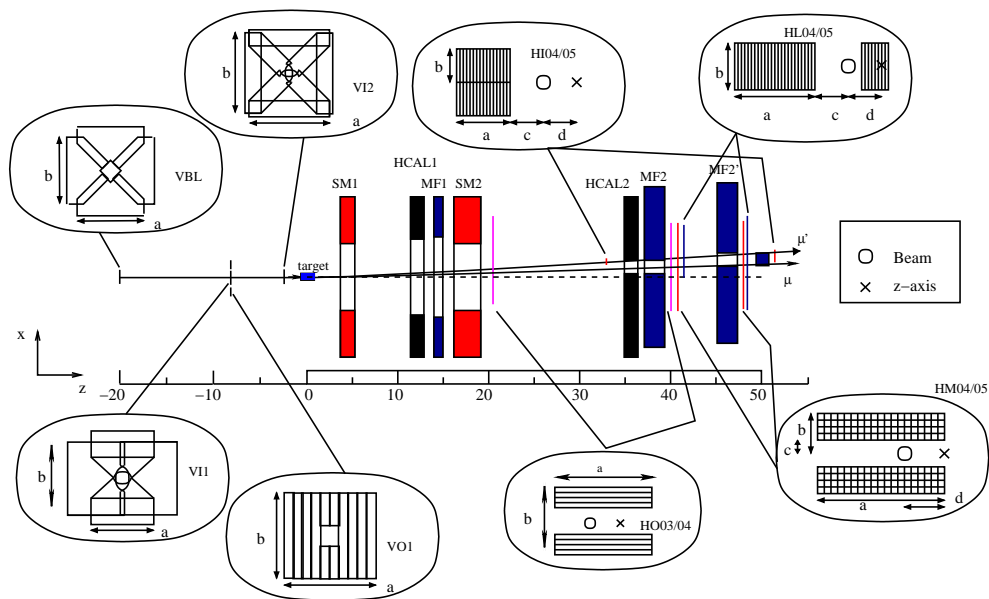


Fig. 31: COMPASS DIS trigger: the various hodoscopes forming the set-up.

$$\text{Trigger: } (H4 * H5) * (HCAL1 \vee HCAL2)$$

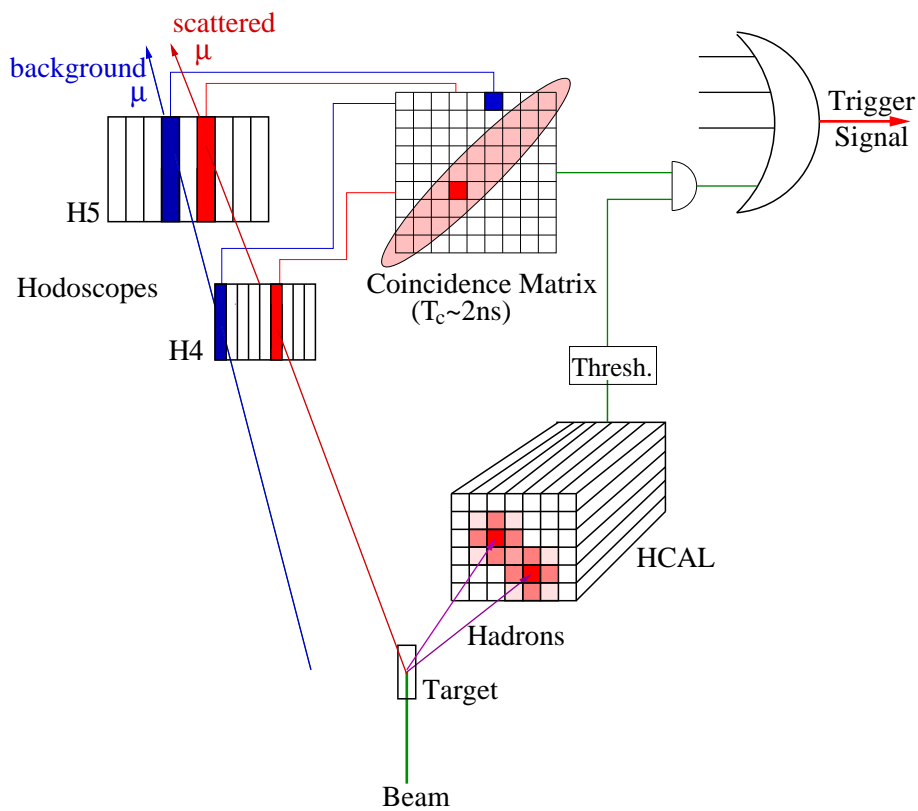


Fig. 32: Scheme demonstrating the working principle of the COMPASS DIS trigger.

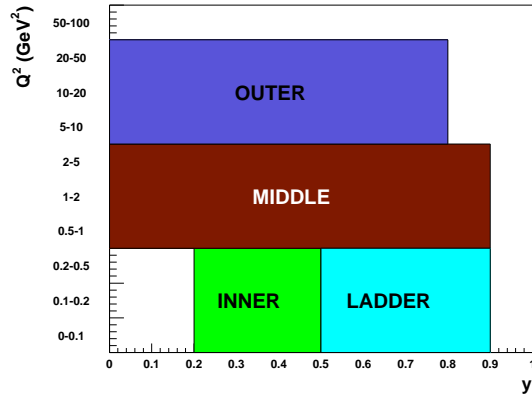


Fig. 33: COMPASS DIS trigger: kinematic regions, in the (y, Q^2) plane, covered by the different combinations of the trigger hodoscopes.

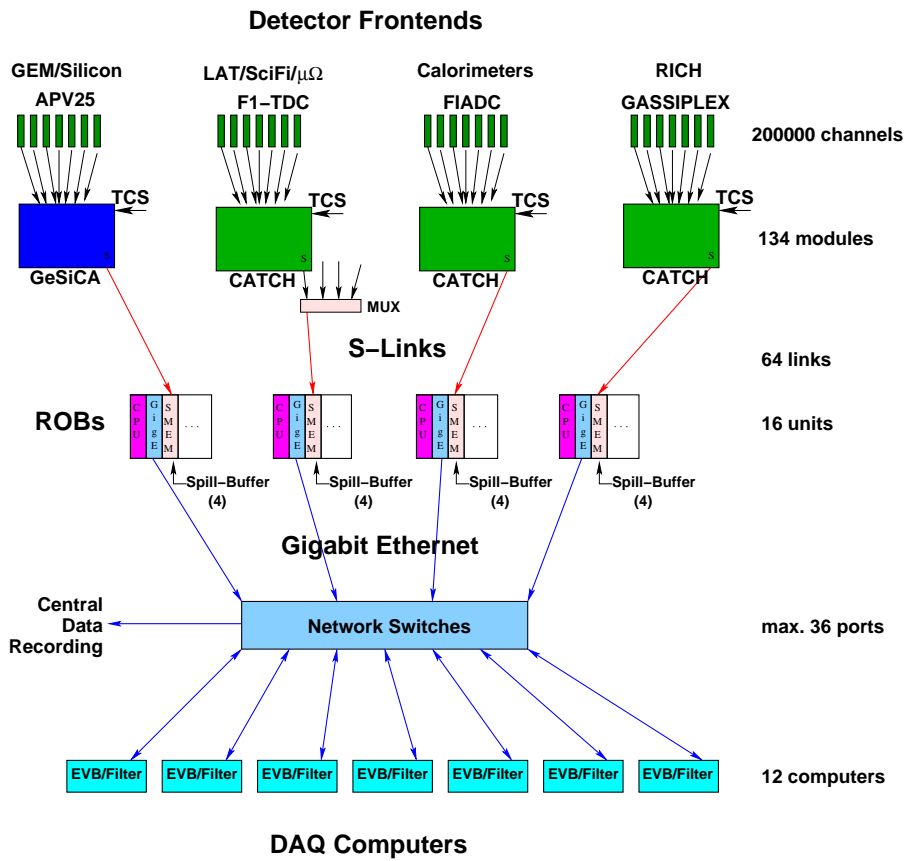


Fig. 34: Overall scheme of the COMPASS read-out and data acquisition system.

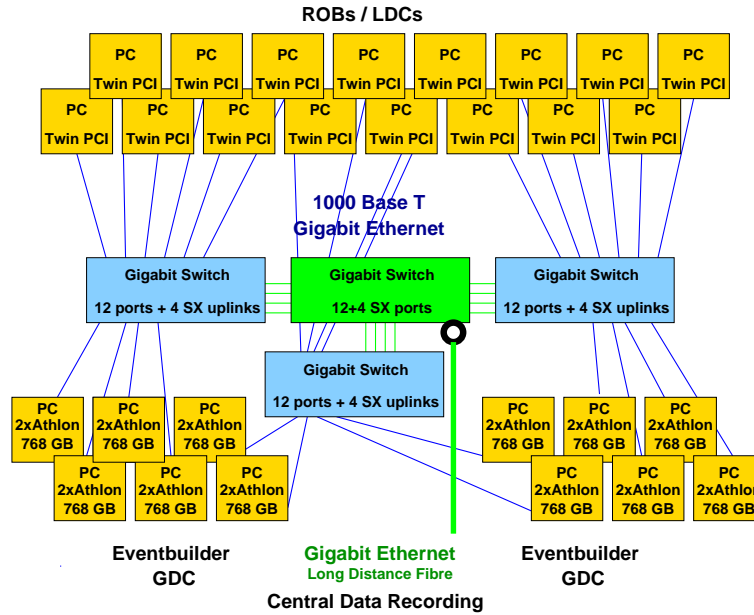


Fig. 35: Scheme of the PC net which forms the heart of the COMPASS data acquisition system.

from front-end and to the spill buffers and 60 MB/s DC downstream of the spill buffers. This figure is comparable with data rates expected for LHC experiments, being only two or three times smaller. Work is in progress to reduce the DAQ dead-time in 2003.

The read-out and DAQ system reached, after the first weeks of the 2002 run period, active time rates of $\sim 85\%$. It was thus possible to collect, during the 2002 run, 260 TB of data, corresponding to 5 billion events. The foreseen figure for the data flow from the COMPASS experiment to the central data recording facility of 3 TB/d was exceeded during the last period of 2002 data taking.

9. COMPLEMENTS OF THE SPECTROMETER

The efficient operation of a modern experiment requires some necessary complementary tools for the slow control of the experimental apparatus and the on-line check of data consistency and quality.

The increasing complexity of experiments and apparatuses and the corresponding enlargement of the collaborations impose efficient, up-to-date solutions for the circulation of information and its availability in real time: the COMPASS electronic log-book is one of the Collaboration instruments answering this challenge.

9.1 The Detector Control System

The aims of the COMPASS Detector Control System (DCS) include

- operator control of hardware systems like the HV and LV ones
- monitoring and data archiving over long-term periods of hardware parameters (such as HV and LV systems, crates, gas systems, pressure and temperature sensors, data taking, cooling systems and data from the SPS accelerator)
- alarm handling and
- information visualisation.

For COMPASS DCS, the Framework package, based on PVSS and designed at CERN for LHC experiments, has been adopted. Data from PC work-stations running Linux and NT systems, from VME CPUs and from fieldbuses (like VME, CANbus, Profibus, serial RS232 lines) are preprocessed.

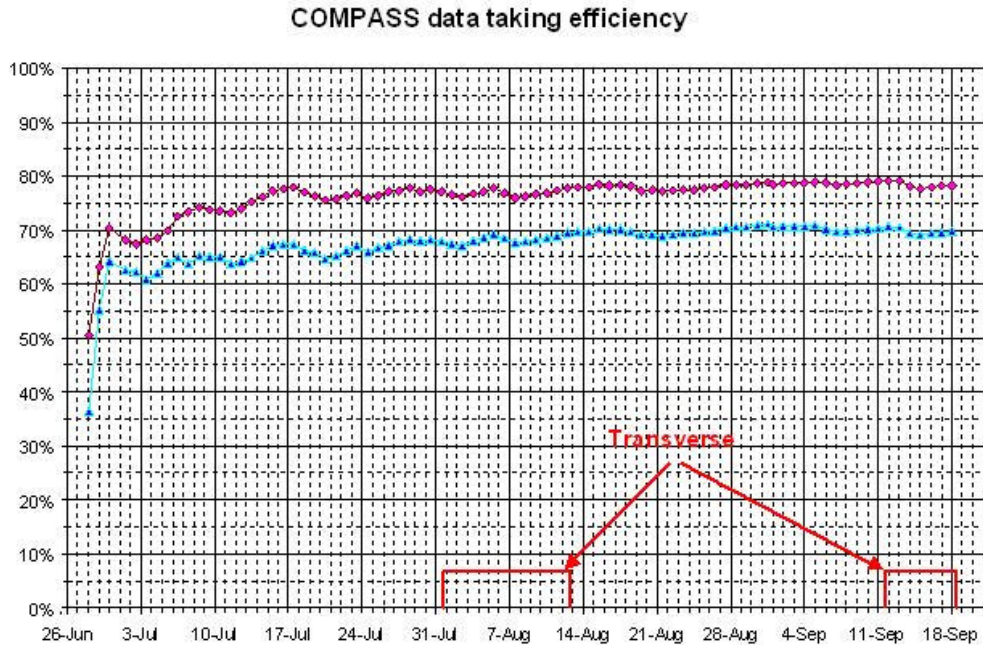


Fig. 36: COMPASS data-taking efficiency during the year 2002 run. The upper curve indicates the integral spectrometer efficiency, the lower curve the integral spectrometer efficiency folded with the SPS efficiency.

The present status can be summarised as follows: the system was started with heavy support from CERN/IT division, several sub-systems are included, but only basic functionality is presently implemented; system optimisation is certainly required to make it more stable and faster.

9.2 The on-line data monitoring system

An up-to-date on-line data monitoring system in COMPASS has been obtained with the COOOL software package written in C++ and built on ROOT libraries. The data decoding libraries are shared with the off-line data analysis package. The data, directly copied from the DAQ farm (more precisely from the event builder PCs), are analysed at a typical rate of ~ 150 (over $\sim 25\,000$) events per burst. Histograms, two-dimensional plots and tables are produced and information correlation as well as on-line cuts can be applied.

The data monitoring is complemented by the MurphyTV package which, by checking data rates and formats from the different hardware sources, allows the prompt diagnostic of the read-out systems.

9.3 The electronic log-book

The electronic log-book, filled on-line by the shift crew during the experiment run, completely replaces the old style paper log-book. Information and comments can be introduced; it is also possible to paste in plots and tables from the on-line monitoring system; data taking information (such as run number, target polarization, number of collected events, information from the SPS) is automatically transferred to the log-book for each 'run' (lasting typically 30 minutes) together with a basic set of monitoring histograms. Collaboration members at CERN can access the information at any time via the world-wide web.

10. CONCLUSIONS

It has been shown that the COMPASS initial lay-out is almost completely implemented and working, while some detector systems are richer than foreseen (scintillating fibres hodoscopes, MWPC stations

and SDC drift chambers). The access to the high Q^2 region, not possible with the foreseen initial set-up, has been opened with the installation of two large-sized W4-5 drift chamber stations (more stations are expected for the 2003 run) and two large-sized trigger hodoscopes.

A few days after the end of the 2002 run, the best summary of the spectrometer performances is given by the figures for the data taking efficiency, shown in Fig. 36. An inspection of the plot clearly indicates an increasing efficiency during the first weeks of data taking and fairly stable performance in the second part of the run period. The mean spectrometer efficiency over the 2002 run is almost 80%; this value, folded with the SPS accelerator efficiency, results in $\sim 70\%$ global efficiency of COMPASS data taking. These performances for efficiency, typical of experiments in operation for many years, demonstrate a largely successful 2002 run.

References

- [1] The COMPASS Collaboration, *Common muon and proton apparatus for structure and spectroscopy*, Proposal to the CERN SPSLC, CERN/SPSLC/96-14, SPSC/P 297, March 1, 1996 and addendum, CERN/SPSLC/96-30, SPSLC/P 297 Add. 1, May 20, 1996.
- [2] J. Ball *et al.*, “First results of the large COMPASS ^6LiD polarized target”, Nucl. Instrum. Meth. A **498** (2003) 101.
- [3] D. Adams *et al.*, Nucl. Instrum. Meth. A **437** (1999) 23.
- [4] J. Bisplinghoff *et al.*, Nucl. Instrum. Meth. A **490** (2002) 101.
- [5] H. Angerer *et al.*, “Present Status Of Silicon Detectors in COMPASS”, Nucl. Instrum. Meth. **512** (2003) 229.
- [6] D. Thers *et al.*, Nucl. Instrum. Meth. A **461** (2001) 29;
A. Magnon *et al.*, Nucl. Instrum. Meth. A **469** (2001) 133;
Ph. Abbon *et al.*, Nucl. Instrum. Meth. A **478** (2002) 210.
- [7] F. Sauli *et al.*, Nucl. Instrum. Meth. A **386** (1997) 531.
- [8] S. Bachmann *et al.*, Nucl. Instrum. Meth. A **470** (2001) 548;
B. Ketzer *et al.*, IEEE Trans. Nucl. Sci. **48** (2001) 1065;
B. Ketzer *et al.*, IEEE Trans. Nucl. Sci. **49** (2002) 2403;
C. Altunbas *et al.*, Nucl. Instrum. Meth. A **490** (2002) 177;
B. Ketzer *et al.*, Nucl. Instrum. Meth. A **494** (2002) 142.
- [9] V.N. Bychkov *et al.*, Physics of Particles and Nuclei, Letters, **2**[111] (2002) 64.
- [10] E. Albrecht *et al.*, “COMPASS RICH-1”, Nucl. Instrum. Meth. A **504** (2003) 354;
G. Baum *et al.*, “RICHONE: a software package for the analysis of COMPASS RICH-1 data”, Nucl. Instrum. Meth. A **502** (2003) 315–317;
E. Albrecht *et al.*, “The mirror system of COMPASS RICH-1”, Nucl. Instrum. Meth. A **502** (2003) 236;
E. Albrecht *et al.*, “The radiator gas and the gas system of COMPASS RICH-1”, Nucl. Instrum. Meth. A **502** (2003) 266.
- [11] RD26 Collaboration, status reports: CERN/DRDC 93-36, 94-49, 96-20.
- [12] The ALICE Collaboration, Technical Design Report of the High Momentum Particle Identification Detector, CERN/LHCC 98-19, ALICE TDR 1, 14 August, 1998.

- [13] F. Piuz, "Rich imaging Cherenkov system based on gaseous photo-detectors: trends and limitations", Nucl. Instrum. Meth. A **502** (2003) 76.
- [14] A. Braem *et al.*, "Technology of photo-cathode production", Nucl. Instrum. Meth. A **502** (2003) 205.
- [15] H. Fischer *et al.*, IEEE Trans. Nucl. Sci., **49** (2002) 443.
- [16] H. Fischer *et al.*, Nucl. Instrum. Meth. A **461** (2001) 507.
- [17] G. Baum *et al.*, Nucl. Instrum. Meth. A **433** (1999) 426;
G. Baum *et al.*, "The COMPASS RICH-1 read-out system", Nucl. Instrum. Meth. A **502** (2003) 246.